2D Covalent Organic Frameworks as Intrinsic Photocatalysts for Visible Light-Driven CO_2 Reduction

Sizhuo Yang,[a] Wenhui Hu,[a] Xin Zhang,[b] Peilei He [a], Brian Pattengale,[a] Cunming Liu,[c] Melissa Cendejas,[d] Ive Hermans,[d,e] Xiaoyi Zhang,[c] Jian Zhang,[b,f]* and Jier Huang [a]*

[a]Department of Chemistry, Marquette University, Milwaukee, Wisconsin, 53201

[b]Department of Chemistry, University of Nebraska-Lincoln, Lincoln, Nebraska, 68588

[c]X-ray Science Division, Argonne National Laboratory, Argonne, Illinois, 60349

[d]Department of Chemistry, University of Wisconsin, Madison, Wisconsin, 53706

[e]Department of Chemical and Biological Engineering, University of Wisconsin, Madison, Wisconsin, 53706

[f]Molecular Foundry, Lawrence Berkeley National Laboratory, Berkeley, California 94720

ABSTRACT: Covalent organic framework (COF) represents an emerging class of porous materials that have exhibited great potential in various applications, particularly in catalysis. In this work, we report a newly designed 2D COF with incorporated Re complex, which exhibits intrinsic light absorption and charge separation (CS) properties. We show that this hybrid catalyst can efficiently reduce CO_2 to form CO under visible light illumination with high electivity (98%) and better activity than its homogeneous Re counterpart. More importantly, using advanced transient optical and X-ray absorption spectroscopy and *in situ* diffuse reflectance spectroscopy, we unraveled three key intermediates that are responsible for CS, the induction period, and rate limiting step in catalysis. This work not only demonstrates the potential of COFs as next generation photocatalysts for solar fuel conversion but also provide unprecedented insight into the mechanistic origins for light-driven CO_2 reduction.

Efficiently capturing CO_2 and simultaneously converting it to chemical fuels driven by solar energy is a promising approach to address energy crisis and climate issues.[1-3] The essential challenge in reaching this elusive goal is to formulate a rationally designed photocatalytic system that can effectively couple a given photosensitizer (PS) with an appropriate molecular catalyst (MC), thereby enabling efficient photosensitization of multi-electron reduction catalysis.[4-6] While many molecular- or semiconductor-based photocatalytic systems have been designed, they all suffer difficulties, such as poor CO_2 adsorption, inappropriate architecture of active sites, rapid charge recombination (CR) or low selectivity etc.[1, 7-9]

As an emerging class of crystalline porous materials, covalent organic frameworks (COFs) represent a versatile platform offering new promise for photocatalytic CO_2 reduction.[10-20] COFs are built from periodic organic building blocks via covalent bond formation, providing an innovative approach for the construction of robust photocatalytic materials with built-in PS (i.e. extended π-conjugation) and MC (e.g. incorporated via postsynthetic modification), thereby facilitating efficient charge separation (CS) and precise determination of the nature of the incorporated MC. Moreover, these structurally diverse materials, with large surface areas and readily tunable pore sizes are expected to provide an ideal scaffold for CO_2 adsorption, diffusion, and activation. However, this undeniable potential has yet to be realized, with some recently studied initial systems

Scheme 1. a) The synthesis of COF and Re-COF. (b) Side view and (c) unit cell of AA stacking COF. (d) Proposed catalytic mechanism for CO_2 reduction.

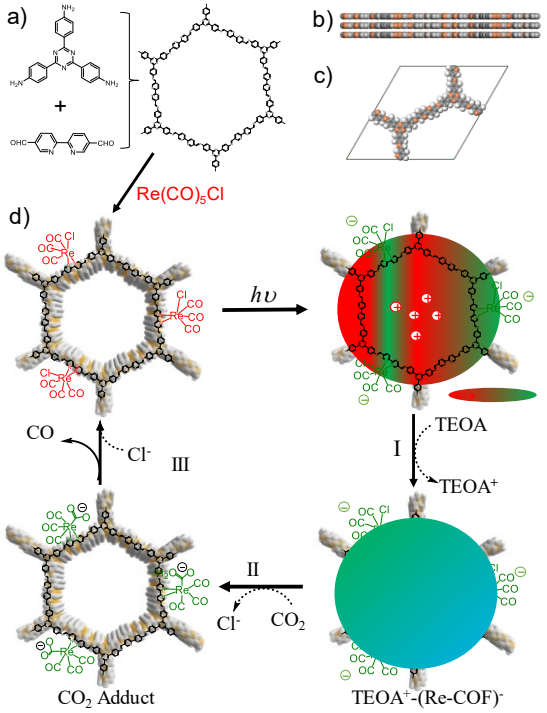

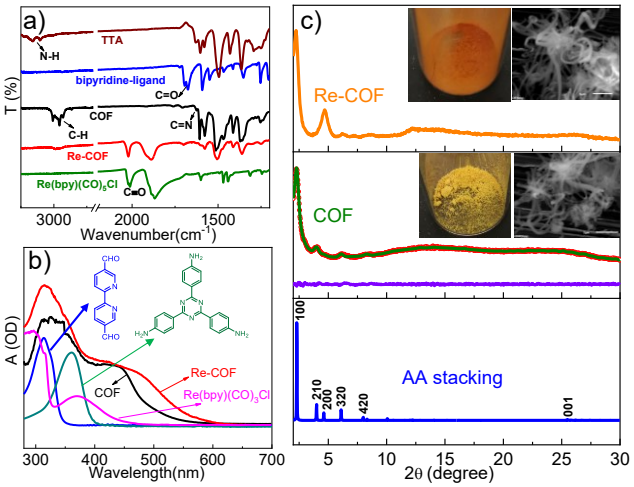

Figure 1. FT-IR (a) and diffuse reflectance UV-visible spectra (b) of COF, Re-COF and their starting materials. (c) Powder XRD patterns of Re-COF and COF obtained experimentally (green), through Pawley refinement (red), and via simulation using AA stacking mode (blue). The purple plot in the middle panel is the difference pattern between experimental and simulated data. The insets are the pictures and SEM images of Re-COF and COF.

exhibiting moderate efficiencies.[21-24] Given the inherent advantages of COFs as photocatalysts and their potential impact on the global energy crisis,[25-29] no time should be wasted in undertaking a well-designed plan to further develop useful devices.

Addressing this pressing need, herein, we report a newly designed COF photocatalyst with a photoactive 2D triazine COF as PS and incorporated tricarbonylchloro(bipyridyl) Re complex ($Re(bpy)(CO)_3Cl$) as CO_2 reduction MC (denoted Re-COF). We show that Re-COF can effectively reduce CO_2 to CO with high selectivity (98%) and durability upon visible light illumination. More importantly, the combination of *in situ* and time-resolved absorption spectroscopy uncovered the key intermediate species that are responsible for CO_2 reduction.

The triazine COF was synthesized from 2,2-bipyridyl-5,5-dialdehyde (BPDA) and 4,4',4''-(1,3,5-triazine-2,4,6-triyl) trianiline (TTA) by solvothermal reactions (Scheme 1a and SI). The formation of imine linkages between aldehyde and TTA in COF was confirmed by FT-IR spectrum (Figure 1a), where we observed the formation of C=N stretching modes at 1626 cm^{-1} that is characteristic of imine in COF and the vanishing of amino band (3213-3435 cm^{-1}) and aldehyde band (1673-1692 cm^{-1}) that were present in TTA and BPDA.[15-16, 30-32] The formation of the COF macrostructure was further supported by the additional absorption band (~ 440 nm) observed in its diffuse reflectance UV-visible spectrum (Figure 1b), which arises from the delocalized intramolecular charge transfer (ICT) band due to π-conjugation of TTA and BPDA.[33-35] Powder XRD patterns of COF show prominent diffraction peaks (Figure 1c), indicating its crystalline nature. The lattice model was simulated using Material Studio 8.0,[30] from which we obtained the most probable structure of COF with AA stacking mode (Scheme 1b and 1c). Pawley refinement of the simulated structure yields XRD patterns that agree well with the experimental data, as indicated by the negligible difference between the simulated and experimental data (middle panel of Figure 1c), suggesting the validity of computational model.

Re moiety was then incorporated into COF via reaction between bipyridine ligand and $Re(CO)_5Cl$ to form Re-COF (Scheme 1a and SI).[36] This is confirmed by the additional peaks at 1887, 1916 and 2022 cm^{-1} in FT-IR spectrum of Re-COF, corresponding to -CO vibrational stretching of $Re(bpy)(CO)_3$ (Figure 1a).[36-38] The XRD patterns (Figure 1c) of Re-COF match well with the simulated data of COF, indicating the preservation of its crystal parameters after Re incorporation. This is further supported by the ^{13}C NMR spectrum (Figure S1) and SEM images (Inset of Figure 1c) of Re-COF and COF. In addition, the local coordination structure of Re in Re-COF measured using X-ray absorption spectroscopy retains that of $Re(bpy)(CO)_3Cl$ (Figure S2 and Table S1), suggesting that $Re(bpy)(CO)_3Cl$ is well preserved in Re-COF. However, it is notable that the UV-visible spectrum of Re-COF are extended to broader region (Figure 1b). This can be attributed to either the vibronic broadening of COFs,[39] or the increased delocalization due to the chelation of $Re(bpy)(CO)_3Cl$. The permanent porosity of COF and Re-COF was confirmed by N_2 sorption measurements at 77 K (Figure S3).

As light absorption and CS are the key initial step to determine whether Re-COF can be used as photocatalyst for CO_2 reduction, we first examined the CS dynamics in Re-COF using transient absorption (TA) spectroscopy following 530 nm excitation (where the TA spectra of $Re(bpy)(CO)_3Cl$ show negligible signal). The TA spectra of COF (Figure 2a) show a positive feature at 600 nm, which can be assigned to the absorption of excited ICT,[41-42] and a negative band centered at 500 nm, which is likely due to stimulated emission (SE)[40-41] (Figure S4) although the contribution from ground state (GS) bleach cannot be com-

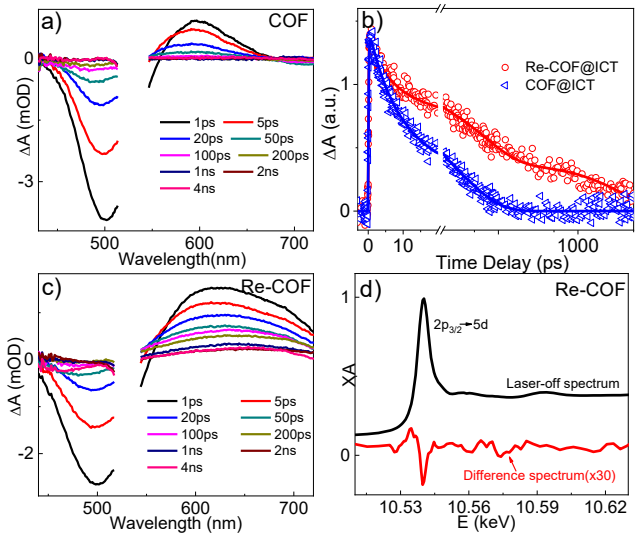

Figure 2. Transient optical spectra of COF (a) and Re-COF (c) following 530 nm excitation. (b) The comparison of kinetics for ICT of COF and Re-COF. (d) The XANES spectrum of Re-COF at Re L_3-edge. The bottom panel is the difference spectrum after subtracting the laser-off spectrum from laser-on spectrum collected at 150 ps delay time.

pletely excluded. The formation (rising component) of the excited ICT (COF@ICT, Figure 2b) is ultrafast with ~200 fs time constant and the CR time is 19.4 ps (Table S2). Compared to that of COF, the TA spectra of Re-COF show a similar SE band and the formation of the excited ICT state (Figure 2c). However, its excited ICT band is much broader than that in COF, which can be attributed to its broader GS spectrum. More interestingly, this excited ICT state of Re-COF (Re-COF@ICT, Figure 2b) exhibits much longer lifetime (τ = 171 ps) than that of COF, suggesting that the incorporation of Re(bpy)(CO)$_3$Cl inhibits CR in Re-COF.

To gain insight on the role of Re(bpy)(CO)$_3$Cl play in elongating the excited ICT lifetime, we directly examined the electron density at the Re center in Re-COF using X-ray transient absorption (XTA) spectroscopy. Figure 2d shows the X-ray absorption near edge structure spectrum of Re-COF collected at Re L$_3$-edge, which is featured by a prominent white line transition corresponding to dipole allowed $2p_{3/2}$-5d transition.[43-44] Also shown in Figure 2d is the difference spectrum obtained by subtracting the GS spectrum from the spectrum collected at 150 ps. The positive signal observed at 10.531 keV directly supports that Re edge shifts to lower energy, suggesting that photoexcitation of Re-COF leads to the reduction of Re center in Re-COF. This is further supported by the negative feature observed at 10.538 keV: the reduction of Re decreased the number of empty d orbitals, prohibiting $2p_{3/2}$-5d transition and thus decreasing its absorption intensity. These results, together with elongated ICT lifetime observed in TA studies, suggest that the electrons in the excited ICT state of Re-COF are partially located in Re(bpy)(CO)$_3$Cl, i.e., electron transfer (ET) indeed occurs from COF to Re(bpy)(CO)$_3$Cl, which explains the retarded CR in Re-COF.

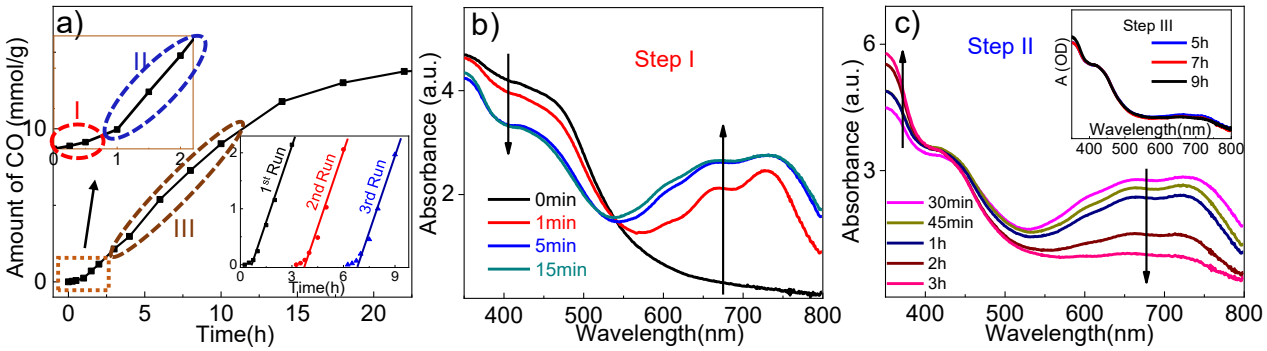

Figure 3. (a) Amount of CO produced as a function of time. The top left inset shows the zoomed in profile in the first 2 hours' reaction, and the lower right inset shows the recyclability of the system after three 3-hour experiments. The *in situ* diffuse reflectance UV-visible spectra of Re-COF under standard photocatalytic conditions within 15 min (b) and 3 h (c). The inset of c shows the *in situ* spectra collected from 5 h to 9 h.

The demonstration of ET from COFs to Re(bpy)(CO)$_3$Cl suggests the feasibility of Re-COF as photocatalysts for solar fuel conversion. Accordingly, we proceeded to examine its photocatalytic activity for CO_2 reduction using TEOA as the sacrificial donor and Xe lamp (cut-off wavelength = 420 nm) as light source. Under the optimized conditions (SI and Figure S5), The system can generate ~15 mmol CO/g of Re-COF steadily for >20 h after ~ 15 min induction period (Figure 3a), accounting for a TON of 48 and 22 times better than its homogeneous counterpart (Figure S5). Since only 2% H_2 was produced in the gas phase (Figure S5), this system has high selectivity for CO_2 reduction to generate CO (98%). Isotopic experiment using $^{13}CO_2$ was performed under the same catalytic conditions. The produced ^{13}CO (m/z = 29) shown by gas chromatography mass spectrometry (Figure S6) confirms that the generated CO comes from CO_2. The recycling experiments after every three hours of reaction show that the catalytic activity persists for at least 3 cycles (lower right inset of Figure 3a).

To gain more mechanistic insight, we collected the *in situ* diffuse reflectance UV-visible spectra of the catalytic system under the catalytic conditions. Immediately following illumination, prominent absorption in 550-800 nm region that resembles the broad absorption of the ICT band in TA was observed (Figure 3b), and can thus be attributed to the formation of the excited ICT state. The intensity of this ICT band increases in the first 15 mins, accompanied by the depletion of absorption at 400-500 nm with an isosbestic point at 539 nm, suggesting that such spectral evolution corresponds to the same process. While similar evolution was observed in the system without CO_2, significantly less evolution was observed in the absence of TEOA (Figure S7), suggesting that reduction quenching of Re-COF by TEOA with the formation of a formal TEOA$^+$-(COF-Re)$^-$ CS state contributes to the evolution. The time window for this spectral evolution agrees with the induction period and can thus be attributed to the accumulation of TEOA$^+$-(COF-Re)$^-$ CS state before catalysis initiates (Step I, Figure 3a).

After the induction period, the absorption at 550-800 nm decreases significantly within 3 h while the feature at < 430 nm grows and a new isosbestic point is observed at 430 nm (Step II, Figure 3c), which results in a distinct feature from Step I and suggests the formation of a new intermediate species. Note that negligible or very slight evolution corresponding to Step II was observed in the system without CO_2 or by replacing Re-COF by COF (Figure S8), suggesting that the intermediate species formed during Step II is associated with CO_2 and Re-moiety. After Step II, the spectral evolution stops (Step III, Figure 3c), consistent with the time window for steady generation of CO, suggesting that the system reaches an equilibrium state.

Taking together, these spectroscopic results point to a mechanistic pathway proposed in Scheme 1d. Upon illumination, the catalytic cycle initiates with the formation of ICT state which is quickly reduced by TEOA, forming a $TEOA^+$-$(COF\text{-}Re)^-$ CS state (Step I). This formal CS state with reduced Re-COF is then able to capture CO_2 to form the next intermediate species (Step II). According to previous literature,[6, 36-38, 45-46] this intermediate species is likely the CO_2 adducts such as $TEOA^+$-$(COF\text{-}Re[CO_2])^-$ or/and $TEOA^+$-$(COF\text{-}Re[CO_2H])^-$, which is formed after the dissociation of Cl^- from Re-moiety. As the spectra persist during steady generation of CO (Step III), the consumption of the CO_2 adducts to eventually form CO represents the rate limiting step of the catalytic reaction.[34-36, 43-44]

In conclusion, we report a newly designed COF hybrid catalyst by incorporating $Re(bpy)(CO)_3Cl$ into 2D triazine COF via postsynthetic modification. We show that this system can efficiently reduce CO_2 with better activity than its homogenous counterpart and high selectivity and stability. Using TA and XTA spectroscopy, we show that this system can undergo facile ICT through ET from photoexcited COF to Re moiety. Using *in situ* diffuse reflectance UV-visible spectroscopy, we unraveled three key intermediate species that are responsible for CS, induction period, and rate limiting step in CO_2 reduction. These results not only demonstrated the great potential of COFs as effective solar fuel photocatalysts but also provided unprecedented new insight into the catalytic mechanism for CO_2 reduction.

ASSOCIATED CONTENT

Supporting Information. The synthesis and standard characterization of $Re(bpy)(CO)_3Cl$, COF, Re-COF, experimental details of transient and *in situ* spectroscopy, ^{13}C NMR of Re-COF, SEM images of COF, fitting parameters for TA and XAS, emission spectra, optimization of photocatalytic reactions, the stability of COF in different solvents, and Re distribution are available free of charge via the Internet at http://pubs.acs.org."

AUTHOR INFORMATION

Corresponding Author

*Jier Huang (jier.huang@marquette.edu)
*Jian Zhang (jzhang3@unl.edu)

Notes

The authors declare no competing financial interests.

ACKNOWLEDGMENT

SY, JH, XZ and JZ thank the support from National Science Foundation (CBET-1706971). Use of the Advanced Photon Source and TEM at Center for Nanomaterials at Argonne National Laboratory was supported by the U. S. Department of Energy, Office of Science, Office of Basic Energy Sciences, under Award No. DE-AC02-06CH11357.

Reference

1. Inoue, T.; Fujishima, A.; Konishi, S.; Honda, K., Photoelectrocatalytic Reduction of Carbon-Dioxide in Aqueous Suspensions of Semiconductor Powders. *Nature* **1979,** *277*, 637-638.
2. D'Alessandro, D. M.; Smit, B.; Long, J. R., Carbon Dioxide Capture: Prospects for New Materials. *Angew. Chem. Int. Ed.* **2010,** *49*, 6058-6082.
3. Appel, A. M.; Bercaw, J. E.; Bocarsly, A. B.; Dobbek, H.; DuBois, D. L.; Dupuis, M.; Ferry, J. G.; Fujita, E.; Hille, R.; Kenis, P. J. A.; Kerfeld, C. A.; Morris, R. H.; Peden, C. H. F.; Portis, A. R.; Ragsdale, S. W.; Rauchfuss, T. B.; Reek, J. N. H.; Seefeldt, L. C.; Thauer, R. K.; Waldrop, G. L., Frontiers, Opportunities, and Challenges in Biochemical and Chemical Catalysis of CO2 Fixation. *Chem. Rev.* **2013,** *113*, 6621-6658.
4. Thoi, V. S.; Kornienko, N.; Margarit, C. G.; Yang, P. D.; Chang, C. J., Visible-Light Photoredox Catalysis: Selective Reduction of Carbon Dioxide to Carbon Monoxide by a Nickel N-Heterocyclic Carbene-Isoquinoline Complex. *J. Am. Chem. Soc.* **2013,** *135*, 14413-14424.
5. Barton, E. E.; Rampulla, D. M.; Bocarsly, A. B., Selective Solar-Driven Reduction of CO2 to Methanol Using a Catalyzed p-GaP Based Photoelectrochemical Cell. *J. Am. Chem. Soc.* **2008,** *130*, 6342-6344.
6. Smieja, J. M.; Benson, E. E.; Kumar, B.; Grice, K. A.; Seu, C. S.; Miller, A. J. M.; Mayer, J. M.; Kubiak, C. P., Kinetic and Structural Studies, Origins of Selectivity, and Interfacial Charge Transfer in the Artificial Photosynthesis of CO. *PNAS.* **2012,** *109*, 15646-15650.
7. White, J. L.; Baruch, M. F.; Pander, J. E.; Hu, Y.; Fortmeyer, I. C.; Park, J. E.; Zhang, T.; Liao, K.; Gu, J.; Yan, Y.; Shaw, T. W.; Abelev, E.; Bocarsly, A. B., Light-Driven Heterogeneous Reduction of Carbon Dioxide: Photocatalysts and Photoelectrodes. *Chem. Rev.* **2015,** *115*, 12888-12935.
8. Wang, S. B.; Yao, W. S.; Lin, J. L.; Ding, Z. X.; Wang, X. C., Cobalt Imidazolate Metal-Organic Frameworks Photosplit CO2 under Mild Reaction Conditions. *Angew. Chem. Int. Ed.* **2014,** *53*, 1034-1038.
9. Wang, S. B.; Wang, X. C., Imidazolium Ionic Liquids, Imidazolylidene Heterocyclic Carbenes, and Zeolitic Imidazolate Frameworks for CO2 Capture and Photochemical Reduction. *Angew. Chem. Int. Ed.* **2016,** *55*, 2308-2320.
10. Diercks, C. S.; Yaghi, O. M., The Atom, the Molecule, and the Covalent Organic Framework. *Science* **2017,** *355*, eaal1585.
11. Waller, P. J.; Gandara, F.; Yaghi, O. M., Chemistry of Covalent Organic Frameworks. *Acc. Chem. Res.* **2015,** *48*, 3053-3063.
12. Bessinger, D.; Ascherl, L.; Auras, F.; Bein, T., Spectrally Switchable Photodetection with Near-Infrared-Absorbing Covalent Organic Frameworks. *J. Am. Chem. Soc.* **2017,** *139*, 12035-12042.
13. Keller, N.; Bessinger, D.; Reuter, S.; Calik, M.; Ascherl, L.; Hanusch, F. C.; Auras, F.; Bein, T., Oligothiophene-Bridged Conjugated Covalent Organic Frameworks. *J. Am. Chem. Soc.* **2017,** *139*, 8194-8199.
14. Dalapati, S.; Jin, E. Q.; Addicoat, M.; Heine, T.; Jiang, D. L., Highly Emissive Covalent Organic Frameworks. *J. Am. Chem. Soc.* **2016,** *138*, 5797-5800.
15. Wan, S.; Gandara, F.; Asano, A.; Furukawa, H.; Saeki, A.; Dey, S. K.; Liao, L.; Ambrogio, M. W.; Botros, Y. Y.; Duan, X. F.; Seki, S.; Stoddart, J. F.; Yaghi, O. M., Covalent Organic Frameworks with High Charge Carrier Mobility. *Chem. Mater.* **2011,** *23*, 4094-4097.
16. Patra, B. C.; Khilari, S.; Manna, R. N.; Mondal, S.; Pradhan, D.; Pradhan, A.; Bhaumik, A., A Metal-Free Covalent Organic Polymer for Electrocatalytic Hydrogen Evolution. *ACS Catal.* **2017,** *7*, 6120-6127.
17. Ma, T. Q.; Kapustin, E. A.; Yin, S. X.; Liang, L.; Zhou, Z. Y.; Niu, J.; Li, L. H.; Wang, Y. Y.; Su, J.; Li, J.; Wang, X. G.; Wang, W. D.; Wang, W.; Sun, J. L.; Yaghi, O. M., Single-crystal X-ray Diffraction Structures of Covalent Organic Frameworks. *Science* **2018,** *361*, 48-52.
18. Ding, S. Y.; Dong, M.; Wang, Y. W.; Chen, Y. T.; Wang, H. Z.; Su, C. Y.; Wang, W., Thioether-Based Fluorescent Covalent Organic Framework for Selective Detection and Facile Removal of Mercury(II). *J. Am. Chem. Soc.* **2016,** *138*, 3031-3037.
19. Jin, E. Q.; Asada, M.; Xu, Q.; Dalapati, S.; Addicoat, M. A.; Brady, M. A.; Xu, H.; Nakamura, T.; Heine, T.; Chen, Q. H.; Jiang, D. L., Two-dimensional Sp(2) Carbon-conjugated Covalent Organic Frameworks. *Science* **2017,** *357*, 673-676.

20. Huang, N.; Wang, P.; Jiang, D. L., Covalent Organic Frameworks: A Materials Platform for Structural and Functional Designs. *Nat. Rev. Mater.* **2016,** *1*, 16068.
21. Lin, S.; Diercks, C. S.; Zhang, Y. B.; Kornienko, N.; Nichols, E. M.; Zhao, Y. B.; Paris, A. R.; Kim, D.; Yang, P.; Yaghi, O. M.; Chang, C. J., Covalent Organic Frameworks Comprising Cobalt Porphyrins for Catalytic CO2 Reduction in Water. *Science* **2015,** *349*, 1208-1213.
22. Yadav, R. K.; Kumar, A.; Park, N. J.; Kong, K. J.; Baeg, J. O., A Highly Efficient Covalent Organic Framework Film Photocatalyst for Selective Solar Fuel Production from CO2. *J. Mater. Chem. A* **2016,** *4*, 9413-9418.
23. Nagai, A.; Chen, X.; Feng, X.; Ding, X. S.; Guo, Z. Q.; Jiang, D. L., A Squaraine-Linked Mesoporous Covalent Organic Framework. *Angew. Chem. Int. Ed.* **2013,** *52*, 3770-3774.
24. Chen, X.; Addicoat, M.; Jin, E. Q.; Zhai, L. P.; Xu, H.; Huang, N.; Guo, Z. Q.; Liu, L. L.; Irle, S.; Jiang, D. L., Locking Covalent Organic Frameworks with Hydrogen Bonds: General and Remarkable Effects on Crystalline Structure, Physical Properties, and Photochemical Activity. *J. Am. Chem. Soc.* **2015,** *137*, 3241-3247.
25. Banerjee, T.; Gottschling, K.; Savasci, G.; Ochsenfeld, C.; Lotsch, B. V., H2 Evolution with Covalent Organic Framework Photocatalysts. *ACS Energy Lett.* **2018,** *3*, 400-409.
26. Banerjee, T.; Haase, F.; Savasci, G.; Gottschling, K.; Ochsenfeld, C.; Lotsch, B. V., Single-Site Photocatalytic H-2 Evolution from Covalent Organic Frameworks with Molecular Cobaloxime Co-Catalysts. *J. Am. Chem. Soc.* **2017,** *139*, 16228-16234.
27. Lin, C. Y.; Zhang, D. T.; Zhao, Z. H.; Xia, Z. H., Covalent Organic Framework Electrocatalysts for Clean Energy Conversion. *Adv. Mater.* **2018,** *30*, 1703646.
28. Pachfule, P.; Acharjya, A.; Roeser, J.; Langenhahn, T.; Schwarze, M.; Schomacker, R.; Thomas, A.; Schmidt, J., Diacetylene Functionalized Covalent Organic Framework (COF) for Photocatalytic Hydrogen Generation. *J. Am. Chem. Soc.* **2018,** *140*, 1423-1427.
29. Sick, T.; Hufnagel, A. G.; Kampmann, J.; Kondofersky, I.; Calik, M.; Rotter, J. M.; Evans, A.; Doblinger, M.; Herbert, S.; Peters, K.; Bohm, D.; Knochel, P.; Medina, D. D.; Fattakhova-Rohlfing, D.; Bein, T., Oriented Films of Conjugated 2D Covalent Organic Frameworks as Photocathodes for Water Splitting. *J. Am. Chem. Soc.* **2018,** *140*, 2085-2092.
30. Ding, S. Y.; Gao, J.; Wang, Q.; Zhang, Y.; Song, W. G.; Su, C. Y.; Wang, W., Construction of Covalent Organic Framework for Catalysis: Pd/COF-LZU1 in Suzuki-Miyaura Coupling Reaction. *J. Am. Chem. Soc.* **2011,** *133*, 19816-19822.
31. Lin, G. Q.; Ding, H. M.; Chen, R. F.; Peng, Z. K.; Wang, B. S.; Wang, C., 3D Porphyrin-Based Covalent Organic Frameworks. *J. Am. Chem. Soc.* **2017,** *139*, 8705-8709.
32. Stegbauer, L.; Schwinghammer, K.; Lotsch, B. V., A Hydrazone-based Covalent Organic Framework for Photocatalytic Hydrogen Production. *Chem. Sci.* **2014,** *5*, 2789-2793.
33. Qian, H. L.; Dai, C.; Yang, C. X.; Yan, X. P., High-Crystallinity Covalent Organic Framework with Dual Fluorescence Emissions and Its Ratiometric Sensing Application. *ACS Appl. Mater. Inter.* **2017,** *9*, 24999-25005.
34. Cho, Y. J.; Lee, A. R.; Kim, S. Y.; Cho, M. J.; Han, W. S.; Son, H. J.; Cho, D. W.; Kang, S. O., The Influence of pi-conjugation on Competitive Pathways: Charge Transfer or Electron Transfer in New D-pi-A and D-pi-Si-pi-A Dyads. *Phys. Chem. Chem. Phys.* **2016,** *18*, 22921-22928.
35. Pop, F.; Riobe, F.; Seifert, S.; Cauchy, T.; Ding, J.; Dupont, N.; Hauser, A.; Koch, M.; Avarvari, N., Tetrathiafulvalene-1,3,5-triazines as (Multi)Donor-Acceptor Systems with Tunable Charge Transfer: Structural, Photophysical, and Theoretical Investigations. *Inorg. Chem.* **2013,** *52*, 5023-5034.
36. Smieja, J. M.; Kubiak, C. P., Re(bipy-tBu)(CO)(3)Cl-improved Catalytic Activity for Reduction of Carbon Dioxide: IR-Spectroelectrochemical and Mechanistic Studies. *Inorg. Chem.* **2010,** *49*, 9283-9289.
37. Hayashi, Y.; Kita, S.; Brunschwig, B. S.; Fujita, E., Involvement of a Binuclear Species with the Re-C(O)O-Re moiety in CO2 Reduction Catalyzed by Tricarbonyl Rhenium(I) Complexes with Diimine Ligands: Strikingly Slow Formation of the Re-Re and Re-C(O)O-Re species from Re(dmb)(CO)(3)S (dmb=4,4 '-dimethyl-2,2 '-bipyridine, S = solvent). *J. Am. Chem. Soc.* **2003,** *125*, 11976-11987.
38. Nganga, J. K.; Samanamu, C. R.; Tanski, J. M.; Pacheco, C.; Saucedo, C.; Batista, V. S.; Grice, K. A.; Ertem, M. Z.; Angeles-Boza, A. M., Electrochemical Reduction of CO2 Catalyzed by Re(pyridine-oxazoline)(CO)(3)Cl Complexes. *Inorg. Chem.* **2017,** *56*, 3214-3226.
39. Qiao, X. X.; Li, Q. Q.; Schaugaard, R. N.; Noffke, B. W.; Liu, Y. J.; Li, D. P.; Liu, L.; Raghavachari, K.; Li, L. S., Well-Defined Nanographene-Rhenium Complex as an Efficient Electrocatalyst and Photocatalyst for Selective CO2 Reduction. *J. Am. Chem. Soc.* **2017,** *139*, 3934-3937.
40. Wang, Y. C.; Jiang, Y. H.; Hua, J. L.; Tian, H.; Qian, S. X., Optical Limiting Properties and Ultrafast Dynamics of Six-Branched Styryl Derivatives Based on 1,3,5-triazine. *J. Appl. Phys.* **2011,** *110,* 033518.
41. Wang, Y. C.; Yin, S. H.; Liu, J. Y.; Yao, L.; Wang, G. Q.; Liu, D. J.; Jing, B.; Cheng, L. H.; Zhong, H. Y.; Shi, X. R.; Fang, Q.; Qian, S. X., Probing Ultrafast Excited State Dynamics and Nonlinear Absorption Properties of Three Star-Shaped Conjugated Oligomers with 1,3,5-triazine Core. *RSC Adv.* **2014,** *4*, 10960-10967.
42. Zhou, Z. N.; Zhou, X. Y.; Wang, X. L.; Jiang, B.; Li, Y. L.; Chen, J. Q.; Xu, J. H., Ultrafast Excited-State Dynamics of Cytosine Aza-Derivative and Analogues. *J. Phys. Chem. A* **2017,** *121*, 2780-2789.
43. Zalis, S.; Milne, C. J.; El Nahhas, A.; Blanco-Rodriguez, A. M.; van der Veen, R. M.; Vlcek, A., Re and Br X-ray Absorption Near-Edge Structure Study of the Ground and Excited States of [ReBr(CO)(3)(bpy)] Interpreted by DFT and TD-DFT Calculations. *Inorg. Chem.* **2013,** *52*, 5775-5785.
44. El Nahhas, A.; van der Veen, R. M.; Penfold, T. J.; Pham, V. T.; Lima, F. A.; Abela, R.; Blanco-Rodriguez, A. M.; Zalis, S.; Vlcek, A.; Tavernelli, I.; Rothlisberger, U.; Milne, C. J.; Chergui, M., X-ray Absorption Spectroscopy of Ground and Excited Rhenium-Carbonyl Diimine-Complexes: Evidence for a Two-Center Electron Transfer. *J. Phys. Chem. A* **2013,** *117*, 361-369.
45. Choi, K. M.; Kim, D.; Rungtaweevoranit, B.; Trickett, C. A.; Barmanbek, J. T. D.; Alshammari, A. S.; Yang, P. D.; Yaghi, O. M., Plasmon-Enhanced PhotoCatalytic CO2 Conversion within Metal Organic Frameworks under Visible Light. *J. Am. Chem. Soc.* **2017,** *139*, 356-362.
46. Abdellah, M.; El-Zohry, A. M.; Antila, L. J.; Windle, C. D.; Reisner, E.; Hammarstrom, L., Time-Resolved IR Spectroscopy Reveals a. Mechanism with TiO2 as a Reversible Electron Acceptor in a TiO2-Re Catalyst System for CO2 Photoreduction. *J. Am. Chem. Soc.* **2017,** *139*, 1226-1232.

TOC